Quantitative assessment of domino effect and escalation scenarios caused by fragment projection

Quantitative Assessment of Domino Effect and Escalation Scenarios caused by Fragment Projection

Alessandro TUGNOLI[1,*], Giordano Emrys SCARPONI[1], Giacomo ANTONIONI[1], Valerio COZZANI[1]

(1) LISES - Dipartimento di Ingegneria Civile, Chimica, Ambientale e dei Materiali
Alma Mater Studiorum - Università di Bologna
via Terracini n.28, 40131 Bologna (Italy)

- REVISED VERSION -

(*) Author to whom correspondence should be addressed.
tel. (+39)-051-2090283; fax (+39)-051-2090247
e-mail: a.tugnoli@unibo.it

Submitted for publication in:
RELIABILITY ENGINEERING AND SYSTEM SAFETY

ABSTRACT

Fragment projection from equipment failure has been extensively recognized as a cause of cascading events and of severe domino scenarios. In recent years several mathematical models suitable for the quantitative assessment of risk due to domino effects and cascading events were developed and validated, but a systematic methodology for quantitative risk assessment caused by fragment projection and impact is still missing. In the present study, a step-by-step approach is proposed for the assessment of domino risk indices due to fragment projection. The approach builds on available sub-models for the quantitative assessment of fragment generation, impact and damage probabilities. Altogether, the proposed model supports a quantification of the risk due to escalation triggered by fragment impact that can be easily automated and integrated in risk assessment studies.

Keywords: fragment projection, fragment impact probability, quantitative risk assessment, cascading events, domino effect, major accident hazard.

NOMENCLATURE

fp	Generic fragmentation pattern
f_P	Frequency of the primary scenario [y^{-1}]
fs	Generic fragment shape
i	Generic index
j	Generic index
k	Generic index
N_F	Number of fragments generated by a given fragmentation pattern
N_{fp}	Number of possible fragmentation patterns for given primary scenario
N_T	Number of potential targets
P_{cp}	Conditional probability of fragment detachment after initial crack propagation
P_{fp}	Conditional probability of the fragmentation pattern fp
P_{fs}	Conditional probability of the considered fragment shape
$P_{gen,j}$	Conditional probability of a given fragment *j* to be generated

$P_{imp,j->i}$	Conditional probability of impact of the fragment *j* on the target *i*
$P_{dam,j,i}$	Conditional probability of damage following the impact of fragment *j* on target *i*
$P_{j->i}$	Overall conditional probability of escalation triggered by a given fragment *j* impacting on the target *i*
$P_{q,f}$	Probability to have a domino scenario corresponding to the f-th permutation of interest
$P_{o,i}$	Overall conditional probability that a target unit is impacted by any of the projected fragments
$\wp_{dir}$	Probability distribution function of the fragment initial direction
$q_{i,j,f}$	Generic permutation
t	Generic index
T^k_t	*t*-th combination of *k* targets
γ	Function
δ	Function
v_{fp}	the total number of domino scenarios considered in the assessment for each fragmentation pattern
v_{fp}	Possible 'partial permutations without repetition' providing a bi-univocal coupling of k fragments to k possible targets
v_k	possible combinations where *k* targets ($k \leq N_F$ and $k \leq N_T$) are simultaneously impacted by k
θ	vertical angle of projection in a polar coordinate system with origin in the fragment source
φ	horizontal angle of projection in a polar coordinate system with origin in the fragment source

1. INTRODUCTION

Fragment projection may occur in the process industry as a consequence of accident scenarios involving the catastrophic failure of process vessels or of fast rotating process equipment [1]. Fragment projection may cause domino effects resulting in cascading events, generating severe secondary accidents [2–5]. This occurs when the projected fragments impact on other equipment items causing the loss of containment of hazardous materials or a severe release of energy. Thus, fragment projection may be considered an escalation vector associated to primary scenarios as confined explosions, boiling liquid expanding vapor explosions (BLEVEs), runaway reactions, and failure of rotating equipment [1,2,6–13].

Domino effect leading to propagation and escalation of a primary accident is a well-known cause of severe accidents in the process industry [14–17]. Events as the Mexico City disaster [18] witness the severity of such scenarios and the death toll they may cause. The risk of escalation is of particular concern in industrial clusters and in extended industrial sites, featuring hundreds and sometimes thousands of equipment items situated in close proximity, and in which relevant quantities of hazardous (e.g., toxic, flammable, etc.) materials are stored or processed [19–24].

Therefore, the assessment and management of risk caused by domino effect and cascading events is a crucial element in the control of major accident hazard in complex industrial parks and infrastructures. Several studies were dedicated in the literature to the quantitative assessment of domino effects and cascading events in industrial facilities and infrastructures, such as power grids [25], water distribution networks [26], and chemical process plants [7,9,27–30]. Even if general frameworks for the quantitative assessment of domino effects are available in the literature (e.g. see [31–33]), less attention was dedicated to the development of quantitative assessment methods to prevent, assess or control the domino scenarios caused by fragment projection.

Nearly any equipment item that isolates a confined volume of fluid may cause accident scenarios involving fragment projection. Thus, the total elimination of fragment projection hazard is not practically feasible in a process plant. Moreover, projection distances of fragments of the order of 1 km were experienced in past events [9,34,35] (up to 3km in a recent event occurred in Tarragona, Spain [36]), hindering the application of safety distance criteria to avoid domino effect [9,35,37,38]. The difficulties in the application of inherent safety concepts to fragment projection scenarios suggests Quantitative Risk Assessment (QRA) methods as the leading approaches to assess, control and reduce the risks related to fragment projection [31,39].

The quantitative assessment of the risk due to fragment projection requires the ability to describe and model, by a comprehensive, systematic and validated approach, all the steps involved in the generation, flight and impact of the fragments. Moreover, the approach should be compatible with other QRA and domino risk assessment techniques. In the last decades, several models applicable to fragment projection were developed. Ballistic models were effectively applied to the calculation of the impact probabilities of a fragment on a given target (e.g. see Baker et al. [40] and later adaptations by many other authors [41–46]). However, the practical application of ballistic models in QRA requires input data on the number, shape and mass of the projected fragments, on the initial projection parameters (e.g. probability density function for the initial projection angles and for the initial projection velocity), and on the probability of damage upon impact.

Probabilistic approaches based on the concept of fragmentation patterns [2,47,48] and on the analysis of extended sets of past accident data were developed to assess the expected number of fragments and fragment drag factors [2,49]. A number of models were proposed to evaluate the initial projection velocity (e.g. [50–55]). More recently, a few studies focused on the definition of suitable probability distributions for the direction of the initial velocity of the fragments [44,45,56,57]. With respect to the damage by missile impact, the literature reports several models for the penetration of metal targets (e.g. asset damage) [1,58–66], while few approaches are available for damage mechanisms different than fragment penetration (indents of pipes [67], fragmentation [68], damage of concrete and brick structures [1]).

As evident from the above cited literature, the complexity of the phenomena involved in fragment projection led to a number of specialized studies of specific topics. Practical approaches to date were mostly based on the extensive adoption of simplified assumptions concerning the number, shape and initial velocity of the fragments, likely to result in over-conservative results. Only few studies strived to provide a systematic approach to the issue (e.g. see [3,45,56,69]). However, a widely accepted procedure for the quantitative assessment of risk due to fragment impact in the framework of industrial risk assessment is still missing.

The present study was aimed at the development of a systematic procedure for the quantitative assessment of the risk of domino scenarios triggered by fragment projection. A comprehensive methodology for the quantitative assessment of risk caused by domino effect was developed by Cozzani and coworkers [34,70] (Figure 1). Though the original methodology already considers different escalation vectors (thermal load, blast wave, etc.), its application to fragment projection was not considered, and specific models, procedures and guidelines allowing its application to fragment projection were not provided. In the present study, the specific sub-models needed for the quantitative assessment of fragment projection as an escalation vector were addressed. The more suitable models to describe the phenomena involved in the fragment projection process, from the identification of the potential sources of fragments to the final probability of escalation, were identified. The models were integrated in order to obtain a coherent flow of information among the steps of the assessment. A specific method allowing the calculation of the expected probability of escalation when the ejection of multiple fragments occurs was calculated. In order to obtain an insight on its potentiality, the methodology was applied to the analysis of a representative case-study in an Oil&Gas facility.

2. METHODOLOGY

The structure of the proposed methodology is outlined in Figure 1. As evident form the figure, it is a multi-step procedure, which unfolds from the identification of the primary events able to trigger domino scenarios to the quantitative assessment of the contribution of domino scenarios triggered by fragments on risk indexes. The input information for the quantitative assessment of escalation is a systematic characterization of the primary risk sources for fragment projection present in the facility of concern. This information can be easily obtained from conventional quantitative risk assessment studies and is usually available when the assessment of escalation and domino effect is undertaken in the context of a more general QRA study.

The general scheme of the methodology is adapted from that proposed by Cozzani et al. [31]. The starting point of the assessment is the identification (by e.g. event tree analysis) of the primary events and related final outcomes and escalation vectors that have a nonnegligible domino potential (step 1 in Figure 1). The single final outcomes and escalation vectors are then analyzed one by one (step 2 and related loop). First, the escalation vector is clearly characterized (step 3): in the case of fragments this provides definition of the shape and number of fragments generated by any of the possible fragmentation patterns. Then follows the identification of possible targets (step 4), the evaluation of domino propagation probability for each target (step 5), and of the consequences from secondary scenarios at the affected target (step 7). Some scenarios with very low probability may be discarded in during the process in order to allow for a quicker assessment (step 6). The risk assessment procedure is then concluded by the calculation of the combined risks from all the assessed final outcomes of primary events (step 8, 9, and 10) and, if desired, of second-level domino events as well (step 11 and related loop).

This general procedure is common to all the potential escalation vectors of concern in the process industry (thermal load, blast wave, fragments). In the following, the specific modifications proposed for fragment projection assessment will be discussed in detail. Particular attention will be devoted to the sub-procedures developed for steps 3 and 5, where the specific characteristics of the fragment escalation vector are taken into account. Further information on the application of the other steps of the procedure and on the assessment of other escalation vectors is widely reported elsewhere [71].

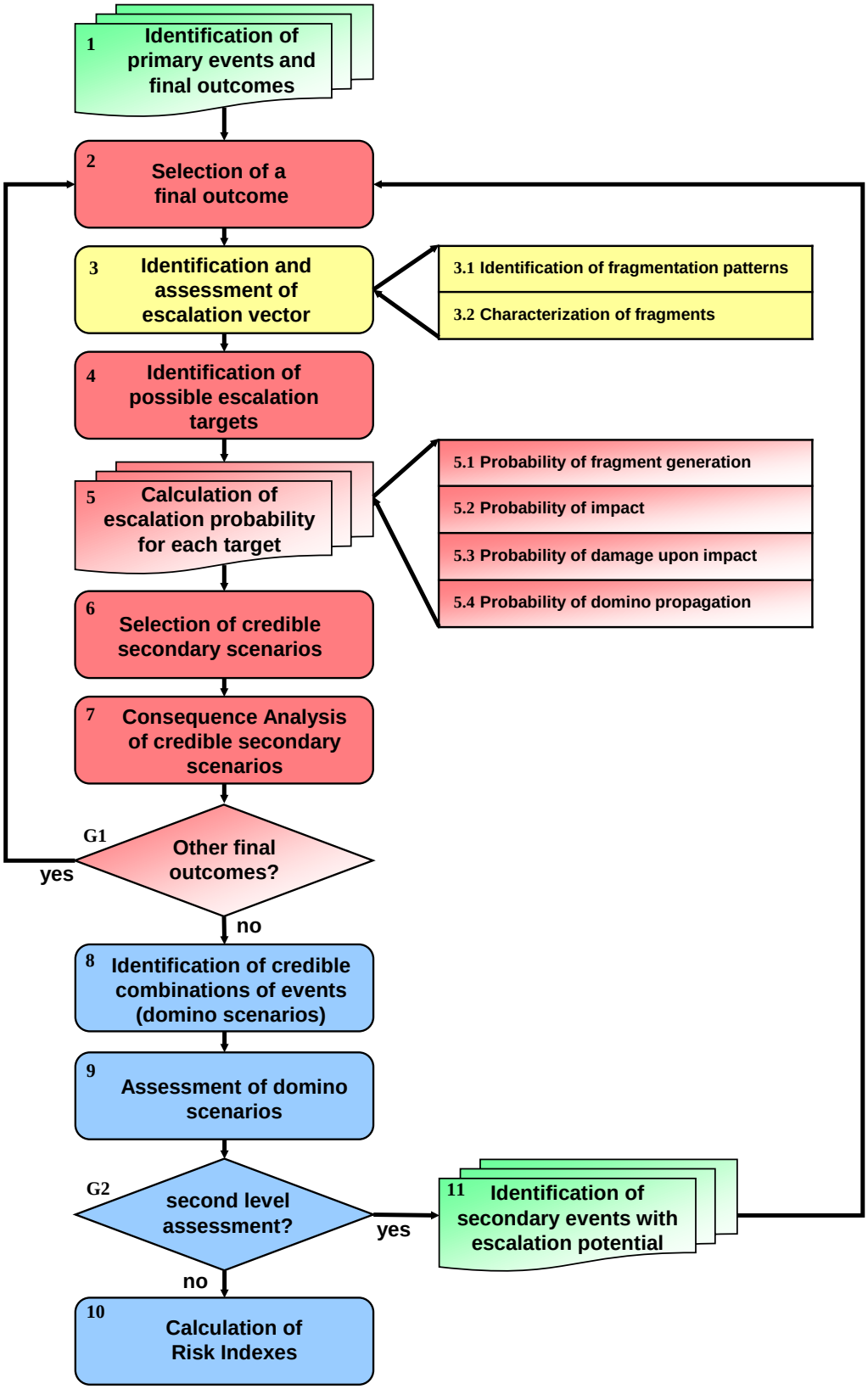

Figure 1. Flow diagram of the proposed methodology for the assessment of risk caused by domino accidental scenarios, reporting a detail of the sub-procedures specific for escalation by fragment projection (step 3 and 5) developed in the present study.

2.1 Identification and assessment of projected fragments as escalation vectors

A critical point in the application of the methodology is the definition of the number and shape of fragments that may be formed and projected in the final outcome of concern of the primary scenario considered (step 3 in Figure 1). Fragments originate when an equipment item undergoes a mechanical failure and part of vessel shell or of connected pipework are physically detached from the original unit. Fragment projection is correlated with accident scenarios which both (i) can generate fragments, and (ii) can transfer to the fragments a sufficient kinetic energy to make them a possible cause of damage to people or equipment. The catastrophic rupture of a vessel is a typical accident scenario resulting in fragment projection, since the release of the internal energy is in part transferred to the vessel fragments as kinetic energy. Fragment projection may also follow the failure of rotating equipment (e.g. compressors, turbines): fragments may be generated by the mechanical failure of moving parts (e.g. blades, sections of rotors), which may detach and pierce through the machine casing.

Though a large number of pieces of equipment in a facility may, at least in theory, be a source of fragments, criteria are required to identify the more likely fragment sources to allow for an effective management of time and computational resources in risk assessment studies. Heuristic criteria for the identification of the more likely fragment sources were proposed by Gubinelli and Cozzani [49] from the analysis of failure mechanics and of a database of more than 180 past accidents. Table 1 reports the proposed criteria for the selection of the more likely fragment sources (the "final outcome" of concern, in step 2 of Figure 1) among the hazardous units identified in a QRA study (step 1). Units that satisfy one or more of the criteria candidate as likely fragment sources.

Vessel-like sources	**Rotating equipment sources**
Accidental scenario triggering fragmentation The primary scenario provides energy for shell fracture (fragment generation) and fragment projection. Credible initiators of fragment projection are the one listed in Table 2.	*Geometrical characteristics* Moving parts in the equipment should have size and mass large enough to provide the momentum necessary to cause damage of the escalation targets. (e.g. discard components with negligible size)
Geometrical characteristics of the equipment Units with the higher volume and/or the higher inventory can provide higher energies for fragment projection. This generates fragments with the momentum necessary to project them at relevant distances and to significantly damage targets.	*Average yearly working time* Rotating components should be operative for a significant number of hours per year. The expected frequency of an event leading to fragment projection is usually proportional to the number of worked hours (e.g. discard rotating equipment in occasional service, such as spare units, start-up auxiliaries, etc.).
Specific operating conditions Units with higher design pressures provide higher energy for projection; units with operating or anomalous conditions enabling scenarios of rapid energy release (BLEVE, run-away, material instability, internal combustion) provide higher energy for projection. This generates fragments with the momentum necessary to project them at relevant distances and to significantly damage targets.	*Specific operating conditions* Moving parts in the equipment should have velocities large enough to provide the momentum necessary to puncture the casing and project them at relevant distances. (e.g. discard low-speed rotating equipment)

Table 1: Heuristic criteria proposed for the identification of potential fragment sources.

Unit taxonomy	Primary accident scenario					
	BLEVE		Physical Explosion	Confined explosion	Runaway reaction	Energetic material decomp.
	Fired	Unfired				
Atmospheric Vessels						
Horizontal Cylindrical Vessel			√	√	√	√
Vertical Cylindrical Vessel			√	√	√	√
Cone-Roof Tank			√	√	(*)	(*)
Other sharp-edged equipment			√	√	(*)	√
Pressurized Vessels						
Horizontal Cylindrical Vessel	√	√	√	√	√	√
Vertical Cylindrical Vessel	√	√	√	√	√	√
Spherical Vessel	√	√	(*)	(*)	(*)	(*)
Other Vessels	√	√	√	√	√	√

Table 2: Possible combinations of accident scenarios and vessel taxonomy which may generate missiles (adapted from Tugnoli et al. [3]). Combination marked as (*), though possible, are unlikely in current industrial practice.

Generation of fragments involves the formation and propagation of cracks through the structural material (usually metal) of the unit. The distribution of these cracks and, consequently, the size and shape of the fragments can be described by a limited set of reference fragmentation patterns, as described by Westin [48]. Gubinelli and Cozzani [49] introduced a correlation between the equipment failure mode, the primary scenario and the number and geometry of projected fragments based on reference fragmentation patterns [2,49]. This approach can be effectively used in step 3.1 of the current methodology (see Figure 1) to associate to each primary scenario a set of N_{fp} fragmentation patterns (*fp*). The fragments originated in each fragmentation pattern can be then characterized (step 3.2 in Figure 1) for their number, shape, weight and drag coefficient. Drag coefficients describe the dissipative forces slowing down the fragment during the flight. A simplified method for the evaluation of this parameter, based on model shapes for the fragments is described by [49].

2.2 Identification of possible escalation targets

Domino risk analysis is usually focused on a limited set of targets with potential for escalating the overall consequences of the accident scenario [71,72]. Target equipment items therefore need to be identified according to the severity of the consequences following the damage by the fragment impact (step 4 of the methodology, see Figure 1). For example, equipment items holding a large inventory of hazardous substances or equipment handling highly toxic material are likely to generate severe secondary scenarios if damaged by impacting missiles. A preliminary identification of these targets may be based on hazard ranking indexes (e.g. Dow F&EI [73], Inherent Safety KPIs [38], etc.) or on the severity of the consequences from the primary scenarios (this is typically available from QRA studies in which the domino assessment is included). An account of this procedure is provided by Cozzani and coworkers [71,72].

The mechanism of escalation by fragment impact is different from that of other escalation vectors (e.g. blast wave and thermal load), and this influences significantly the evaluation of the escalation probability (Figure 2). Blast waves and thermal loads are "field-like" escalation vectors, where a portion of the space is interested by the vector and all the targets in that area can be damaged. In these cases, the damage of a target by the escalation vector does not affect the possibility of the vector itself to damage other target in the affected area.

Differently, escalation by fragments occurs by a "one-to-one" escalation mechanism: a given fragment that impacts on a target cannot impact, at the same time, on any other spatial location. Hence, a given fragment may affect only a single target at a time, provided that the distances among the potential targets and between the fragment source and the targets are sufficiently large. Ricochet is usually neglected for fragmentation accidents, due to reduced kinetic energy of the fragment after the first impact (i.e. small probability of effective damage on a secondary target). As a result, the number of fragments generated simultaneously by a FP provides an upper bound to the number of targets that can be affected in a domino fragmentation scenario.

For the purpose of escalation probability calculation (step 5) and of consequence analysis of escalation scenarios (step 7) it is important to identify all the sets of possible combinations of targets that can be affected by a fragmentation event (i.e. the domino scenarios). Each fragmentation pattern identified at step 3.1, produces a different set of fragments (different number, different characteristics) and will be considered as a separate case in the following. If N_F fragments are generated at the same time by a given fragmentation pattern and N_T potential targets of concern are identified, the possible combinations where k targets ($k \leq N_F$ and $k \leq N_T$) are simultaneously impacted by k different fragments are:

$$\nu_k = \frac{N_T!}{(N_T - k)! \cdot k!} \tag{1}$$

Since k may assume different values within the limits given above, the total number of domino scenarios considered in the assessment for each fragmentation pattern is:

$$\nu_{fp} = \sum_{k=1}^{min(N_F,N_T)} \nu_k = \sum_{k=1}^{min(N_F,N_T)} \frac{N_T!}{(N_T-k)! \cdot k!} \tag{2}$$

where the subscript *fp* indicates the fragmentation pattern of interest. The combinations above do not take into account which specific fragment, among those generated, impacts

on any given target. Due to the "one-to-one" nature of the fragment escalation vector, the assessment of the escalation probabilities for each of the combinations above requires the study of all the possible couples of fragment and affected target.

For any given t-th combination (T^k_t) where k targets are affected by fragments from a given fragmentation pattern (*fp*), there are $\nu_{F,k}$ possible 'partial permutations (or arrangements) without repetition' providing a bi-univocal coupling of k fragments to k possible targets:

$$\nu_{F,k} = \frac{N_F!}{(N_F - k)!} \tag{3}$$

where N_F is the number of fragments generated by the fragmentation pattern of interest.

Equation (3) is strictly valid if only one fragment impacts on any selected target. Considering permutations, the impact of multiple fragments on a single target is possible. However, this it would largely increase the number of cases to be considered in the assessment, without appreciably changing the numerical results of the evaluation. Actually, considering the phenomena governing the fragmentation of a vessel, when a limited number of fragments is generated in the primary event, the probability that two or more fragments impact on the same target, at least in the far field, is sufficiently small to be practically negligible [44]. It should also be remarked that, if probability of damage upon impact at step 5.3 is conservatively assumed to be equal to 1 (as in several proposed literature approaches), multiple fragment impacts have no interest, since any successive impact after that of the first fragment considered will not further increase the damage probability of the target.

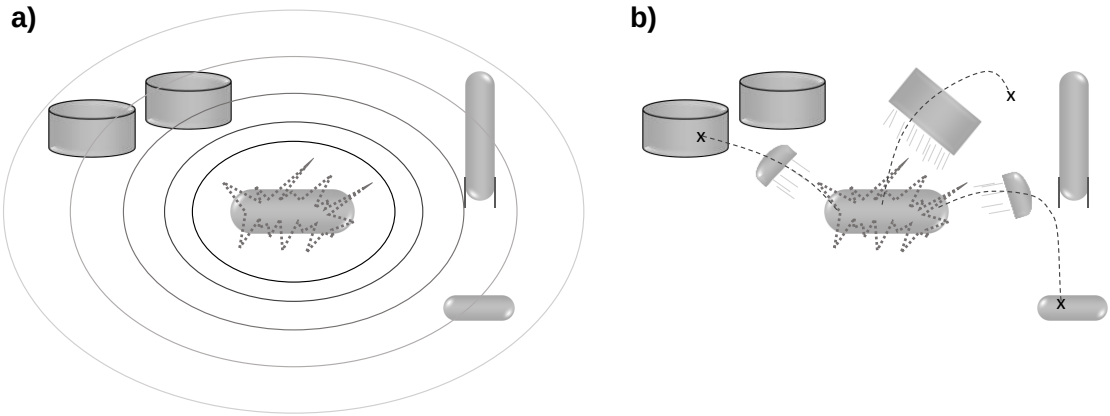

Figure 2. Representation of the escalation mechanism by different types of escalation vectors: a) "field-like" escalation vectors (thermal load, blast wave); b) fragment projection.

2.3 Calculation of escalation probability

The calculation of the escalation probability caused by fragments (step 5 in the methodology, see Figure 1) needs to be carried out considering the chain of events of the impact mechanism (fragment generation, fragment impact, and target damage). First, each phenomenon in the chain is assessed in probabilistic terms for any possible couple of fragment and target. Then, the results are combined in order to evaluate the probability of the possible escalation scenarios.

2.3.1 Probability of fragment generation

The probability of a given fragment *j* to be generated, ($P_{gen,j}$), quantifies the conditional probability that a fragment with a given shape and mass (as identified in step 3.2) is formed and projected given the primary event (step 5.1 in Figure 1). It is calculated from the combination of the probabilities of the phenomena involved:

$$P_{gen,j} = P_{cp} \cdot P_{fp} \cdot P_{fs} \tag{4}$$

where P_{cp} is the conditional probability of fragment detachment after initial crack propagation, P_{fp} is the conditional probability of the fragmentation pattern of concern, P_{fs} is the conditional probability of the considered fragment shape.

As discussed in Gubinelli and Cozzani [49], crack propagation may arrest, without producing any detached fragment. The analysis of past accident data allowed obtaining the data for the probability of fragment generation after initial crack propagation (P_{cp}) [47,49,74].

The conditional probability for a fragmentation pattern (P_{fp}) to occur given vessel fragmentation can be evaluated by past accident data. Conditional probabilities for reference fragmentation patterns and fragment number may be obtained from the literature [49]. A more accurate assessment of the fragmentation mechanism may be obtained performing a stress analysis of the vessel under consideration [75,76]. However, the level of detail and the computational resources required to carry out this assessment are unaffordable in the framework of a QRA of an industrial facility.

In some fragmentation accidents, during equipment failure, one of the final fragments may assume different shapes due to (e.g. flattened or non-flattened). The conditional probability of fragment shape (P_{fs}) is relevant for capturing this phenomenon. Statistical data can be found in the study by Gubinelli and Cozzani [49].

2.3.2 Probability of impact

As remarked by Mannan [1], the flight of a fragment is a standard problem in mechanics, for which a fundamental approach is described by Baker et al. [50]. The probability of impact of a fragment on a target with a given geometry can be calculated by the model proposed by Gubinelli et al. [44] for the assessment of the probability of domino scenarios caused by fragment impact (step 5.2 in Figure 1). The methodology is based on a ballistic analysis of all the possible trajectories of a fragment with a given mass, shape and initial velocity. A comparison with data available in the literature [47,50] provided a validation of the model.

The model inputs are the initial conditions of the generated fragment (direction and velocity), the fragment characteristics (shape, dimensions, weight) and the characteristics of the target (dimension and location). The impact among a flying fragment and a target occurs under a limited range of initial projection angles. The presence of barriers aimed at intercepting the fragments (such as walls) can further reduce the extension of such range [77]. The total impact probability of the fragment j on the target i may be thus expressed as follow:

$$P_{imp,j->i} = \int_{\Delta\theta} \int_{\Delta\varphi} \wp_{dir}(\theta,\varphi) \cdot d\theta \cdot d\varphi \quad (5)$$

where $\wp(\theta,\varphi)$ is the probability distribution function of the fragment initial direction, θ and φ are respectively the vertical and horizontal angles of projection in a polar coordinate system with origin in the fragment source, and Δθ and Δφ are the intervals of vertical and horizontal angles for which the impact of j on i takes place.

Tugnoli et al. [78] proposed a set of validated probability distribution functions for the initial angles, considering different categories of equipment. Other values, specific for horizontal cylindrical storage vessels are reported by Pula et al. [57], Mébarki et al. [45] and Nguyen et al. [56].

With respect to the initial velocity of the fragment, this may be evaluated from the kinetic energy transferred to the fragments during vessel failure [55]. The best model to describe initial velocity is usually identified on the basis of the primary event triggering fragmentation. According to TNO's Yellow Book [79], the Baker model [50] and/or the Gel'fand model [53] are suggested for physical explosion scenarios. The Baum's formula [80] is suggested for BLEVEs. The Gel'fand's method [53] best applies to runaway reactions and internal explosions. The Moore's relation [54] is the more adequate for vessel burst with high scaled pressures and decomposition of energetic materials. Initial velocity of the fragment from rotating equipment can be conservatively assumed equal to the maximum tangential velocity of the rotor before fragmentation or can be estimated assuming the conservation of the kinetic energy of the detached section. A specific reduction of the initial velocity may be considered in order to take into account the energy required for casing perforation.

Finally, the solution of the ballistic equation requires information on the drag factor of the airborne fragment. The procedure described by Gubinelli et al. [44] can be applied to this purpose.

2.3.3 Probability of damage upon impact

The probability of irreversible effects following target impact, or conditional probability of damage ($P_{dam,j,i}$), defines the vulnerability of the target (step 5.3 in Figure 1). The impact of a fragment on a piece of equipment can damage the target either by penetration or by plastic collapse. Consequences on the target in terms of possible loss of containment are generally different. A penetrating fragment may pierce a hole through the shell of the target and initiate a continuous or semi-continuous release. A high mass non-penetrating fragment may cause significant deformations of the target, possibly leading to the catastrophic collapse and to the instantaneous release of its entire content.

Though several models are available for the calculation of fragment penetration on a given target, no criteria are provided to date for the estimation of the actual damage probability. The comparison of the penetration depth with the actual thickness of the target may provide a step function for damage probability. Fragment penetration depth in metal targets can be evaluated according to the fragment shape and kinetic energy (required inputs are available respectively from step 3.2 and 5.2 of the procedure) by a number of models applicable to metal targets (e.g. Baker et al. [61] for large size

fragments, Gwaltney et al. [81] or Ohte et al. [59] for small size fragments). Clearly enough, target protection barriers may be accounted for, if present [82,83].

Alternatively, a typical conservative hypothesis widely used in the literature is to assume a value equal to 1 for the damage probability if the impact takes place [1].

2.3.4 Probability of domino propagation

The overall conditional probability of escalation triggered by a given fragment j impacting on the target i ($P_{j->i}$) is the product of the three contributions calculated above:

$$P_{j->i} = P_{gen,j} \cdot P_{imp,j->i} \cdot P_{dam,j,i} \qquad (6)$$

Where $P_{gen,j}$ is the probability of each fragment to be generated, $P_{imp,j->i}$ is the probability of impact on the target i, and $P_{dam,j,i}$ is the probability of damage following target impact.

As discussed in section 2.3, given a set of k targets (T^k_t) there are $\nu_{F,k}$ possible partial permutations coupling the k impacting fragments of a fragmentation pattern (*fp*) and the k impacted targets. Each these permutations can be represented in a three-dimensional matrix ($q_{i,j,f}$):

$$q_{i,j,f} = \begin{cases} 1 & \text{if j-th fragment impacts on i-th target in f-th permutation} \\ 0 & \text{otherwise} \end{cases}$$

with $i \in [1, N_T]$ target identifier, $j \in [1, N_F]$ fragment identifier, $f \in [1, \nu_{F,k}]$ permutation identifier.

A domino scenario corresponding to a given permutation occurs if: i) all the k fragments of concern impact on the desired k targets, and ii) none of the other N_F-k fragments impacts on any of the other N_T–k targets. The probability to have a domino scenario corresponding to the f-th permutation of interest ($P_{q,f}$) may then be calculated combining the probability of the escalation for the single couple fragment-target (step 5.4 in Figure 1). Under the assumption that a fragment can impact only on a single location, the probability $P_{q,f}$ can be evaluated as:

$$P_{q,f} = \prod_{i=1}^{N_T} \prod_{j=1}^{N_F} \left[\delta(q,i,j,f) \cdot P_{j->i} + \gamma(q,i,j,f) \right] \qquad (7)$$

Where $P_{j->i}$ is the probability of escalation triggered by a given fragment j impacting on the target i, and $\delta(q,i,j)$ and $\gamma(q,i,j)$ are functions defined as:

$$\delta(q,i,j,f) = \begin{cases} 1 & \text{if } q_{i,j,f} = 1 \\ -1 & \text{if } \forall a \in [0, N_T] \; q_{a,j,f} = 0 \text{ and } \forall b \in [1, N_F] \; q_{i,b,f} = 0 \\ 0 & \textit{otherwise} \end{cases} \qquad (8a)$$

$$\gamma(q,i,j,f) = \begin{cases} 0 & \text{if } q_{i,j,f} = 1 \\ 1 & \text{if } \forall a \in [0, N_T] \; q_{a,j,f} = 0 \text{ and } \forall b \in [1, N_F] \; q_{i,b,f} = 0 \\ 1 & \textit{otherwise} \end{cases} \qquad (8b)$$

If targets are located at some distance from the primary source, the probability of damage $P_{j->i}$ are relatively small numbers. In these cases, the terms of Eq. (7) corresponding to the

probability of not having any fragment impacting on unwanted targets is very close to 1. Therefore, Eq. (7) can be simplified as follows:

$$P_{q,f} = \prod_{i=1}^{N_T} \prod_{j=1}^{N_F} \left[q_{i,j,f} \cdot P_{j->i} + (1 - q_{i,j,f}) \right] \quad (9)$$

The $\nu_{F,k}$ possible 'partial permutations without repetitions' for a given combination of k targets (T^k_t) and a given fragmentation pattern (*fp*) are, by definition, mutually exclusive events: hence the probability to have a domino scenario affecting the set T^k_t from the fragmentation pattern (*fp*) is:

$$P_{T_t^k}^{fp} = \sum_{f=1}^{\nu_{F,k}} P_{q,f} \quad (10)$$

Since also the alternative fragmentation patterns for a unit are mutually exclusive events, the probability to have the domino scenario affecting the set T^k_t from any fragmentation pattern is:

$$P_{dom,T_t^k} = \sum_{fp=1}^{N_{fp}} P_{T_t^k}^{fp} \quad (11)$$

2.4 Secondary scenarios and consequence assessment

After the escalation probability has been assessed, the secondary scenarios need to be identified (step 6 in the procedure, see Figure 1). An escalation leading to a domino scenario is based on the damage of a set T^k_t of targets. As discussed with respect to the probability of damage (step 5.3), no specific model is available to date for the quantification of the damage mode and intensity. A typical conservative assumption, especially in the case of large fragments, is that the impact leads to the collapse of the structure, with a consequent catastrophic loss of containment. A less conservative assumption considers the formation of a breach with the same size of the greater dimension of the impacting fragment. Specific considerations should be introduced if structural elements of the target are damaged, since in such scenarios collapse may follow local damage as well.

The consequences of the loss of containment of hazardous materials in the secondary scenario need then to be assessed (step 7 in Figure 1). These can be described by conventional event tree analysis, taking into account that the primary scenario may affect the possible consequences (e.g. an ignition source may be easily available). The identification and analysis of a single scenario for the secondary consequences is a simplifying assumption that may be introduced to reduce the computational burden for the risk evaluation. Scenario prioritization criteria may be applied, as described in Cozzani et al. [31].

The following steps in the assessment procedure (steps from 8 to 11 in Figure 1) are not specific of the procedure for the calculation of the probability of escalation caused by fragments, being the same for the calculation of probability of any other escalation vector, and are described in detail in previous publications [31,71].

3. Case Study

The proposed methodology was applied to a case study concerning an upstream Oil&Gas installation. A fictitious lay-out of a plant section of an offshore production facility was derived from the actual design documents of an existing plant in very shallow waters, e.g. as those operating in the Caspian Sea. The plant section was considered as part of a greater installation comprising wellheads, three-phase separation, sweetening and gas compression. The section layout unfolds on a single level. It is part of the greater three-phase separation section of the plant and comprises of several units (separators, utility tanks, etc.) as shown in Figure 2.

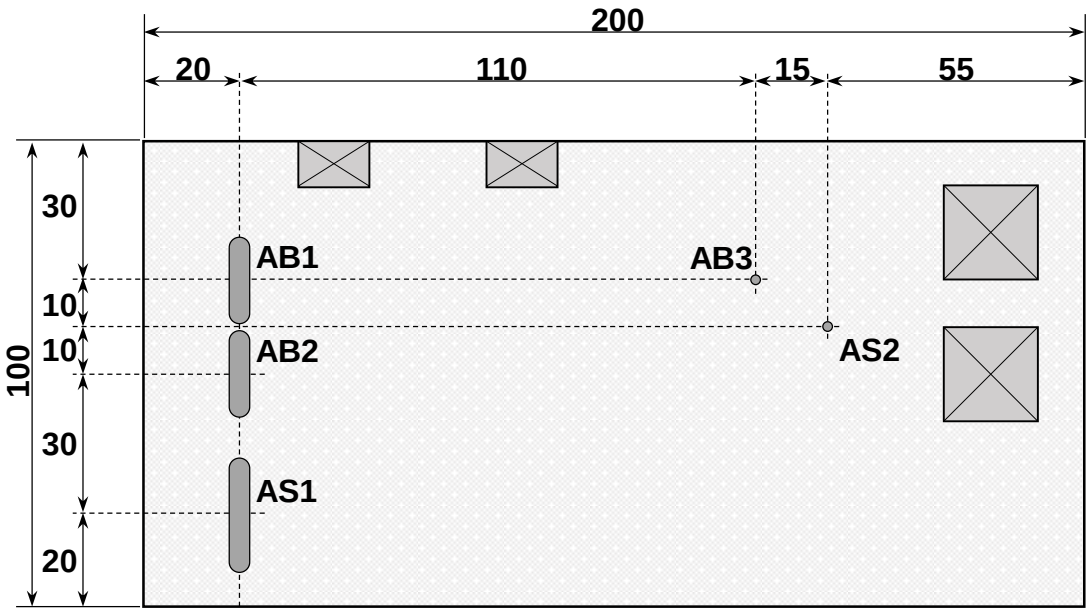

Figure 2: layout of the facility considered in the case study (distances are in m)

The case of fragments originated by unit AS2 is considered in the following. Unit AS2 is a vertical cylindrical vessel containing pressurized inert gas (Table 3). The hazard identification study of the unit, carried out applying Hazard and Operability Analysis, pointed out the possibility of catastrophic failure of the unit, originating a mechanical explosion (blast wave) and fragment projection. This scenario is considered as the primary event causing fragment projection.

Potential domino targets considered are nearby units AB1, AB2, AB3 and AS1. The main characteristics of these units are presented in Table 3. The units hold flammable gas and gas-liquid mixtures. In case of damage of these units by the impact of fragments from AS2, a loss of containment scenario is expected. Different secondary scenarios may take place in case of fragment impact (depending on both the damage experienced by the target unit – piercing or catastrophic failure – and on the events following the release - immediate or delayed ignition, etc.). However, in the present study, for the sake of simplicity, due to the demonstrative aim of the case study, in analogy with the approach proposed by Cozzani et al. [31], a single secondary scenario is associated to each unit. Table 3 reports the secondary scenarios considered for each unit.

ID	AS2 (fragment source)
***Thickness* [mm]**	15
***Operative T* [°C]**	50
***Operative P* [bar]**	10
Reference Substance	Nitrogen
Primary event	Mechanical explosion
***f_P* [ev./yr]**	$5 \cdot 10^{-5}$

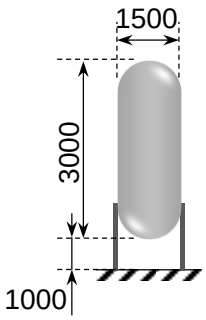

ID	AB1 and AB2 (fragment target)
***Thickness* [mm]**	15
***Operative T* [°C]**	70
***Operative P* [bar]**	30
Reference Substance	Propane
Secondary event	Fireball

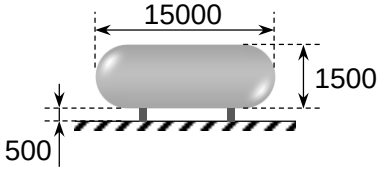

ID	AB3 (fragment target)
***Thickness* [mm]**	15
***Operative T* [°C]**	60
***Operative P* [bar]**	9
Reference Substance	Methane
Secondary event	Flash fire

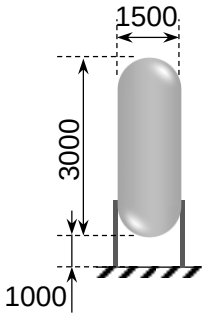

ID	AS1 (fragment target)
***Thickness* [mm]**	50
***Operative T* [°C]**	85

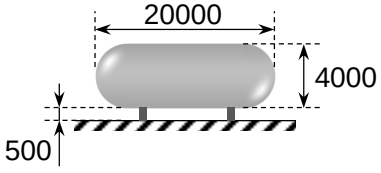

***Operative P* [bar]**	95	
Reference Substance	Propane	
Secondary event	Fireball	

Table 3: Main characteristics of reference equipment considered in the case study (dimensions are in mm)

4. Results and discussion

4.1 Results of the case study

In the analysis of the case-study, unit AS2 was considered the source generating the fragments considered in the risk assessment (steps 1 and 2). Actually, the catastrophic failure (mechanical explosion) of unit AS2 may result in a blast wave and fragment projection. The direct consequences of the blast wave are expected to be minor. At distances greater than 13m, the peak overpressure, as calculated by the TNT model based on energy from the isentropic expansion of gas [84], is below the escalation threshold for atmospheric equipment proposed by Cozzani et al. [34], corresponding to 16 kPa. This suggests that no significant domino effect can be caused by the blast wave. Local specific individual risk caused from the blast wave, calculated using the probit model proposed by [85], dramatically decreases with the distance from the source (Figure 4-a), suggesting minor contributions to the overall risk of the facility.

Nevertheless, the burst of unit AS2 is also a possible cause of fragment projection, which may impact nearby units and trigger domino scenarios. As shown in table 4, three main fragmentation patterns are likely for the vessel on the basis of the study of Gubinelli and Cozzani [49] (step 3.1). Fragmentation patterns FP1 and FP2 are very similar, the difference being if the crack propagation occurs in the lower (FP1) or in the upper (FP2) portion of the vessel. Both lead to the formation of 2 fragments. Fragmentation pattern FP3 produces 3 fragments. Dimensions and weight of the fragments were evaluated for each fragmentation pattern (step 3.2) based on the size of vessel AS2, and are reported in table 5.

Several units in the lay-out considered are potential targets for escalation caused by fragments generated from unit AS2 (step 4). As a matter of fact, the maximum distance that can be reached by these fragments was estimated to be 424 m (see step 5.2), well beyond separation distances of the units. Hence, all the units identified in table 3 should be considered as potential targets (N_T=4), since they contain hazardous materials and, if impacted, may originate severe secondary scenarios.

fp	N_F	***K=1*** ν_k**=4**	***k=2*** ν_k**=6**	***k=3*** ν_k**=4**	ν_{fp}
FP1	2	$\nu_{F,k}$=2	$\nu_{F,k}$=2	N/A	10
FP2	2	$\nu_{F,k}$=2	$\nu_{F,k}$=2	N/A	10
FP3	3	$\nu_{F,k}$=3	$\nu_{F,k}$=6	$\nu_{F,k}$=6	14

Table 4: Number of target combinations (ν_k) and fragment-target partial permutations ($\nu_{F,k}$) considered impact probability calculations in the presented case study (N_T=4).

	Size	**Mass**	**Drag factor** [49]
FP1-TE	Diameter = 1.5 m Length = 3.7 m	420 kg	$6.9 \cdot 10^{-3}$
FP1-PL	Diameter = 2.3 m	80 kg	$3.3 \cdot 10^{-2}$
FP2-TE	Diameter = 1.5 m Length = 0.7 m	80 kg	$6.9 \cdot 10^{-3}$
FP2-PL	Diameter = 2.3 m	80 kg	$3.3 \cdot 10^{-2}$
FP3-TE1	Diameter = 1.5 m Length = 0.7 m	80 kg	$6.9 \cdot 10^{-3}$
FP3-PL	Sides = 4.7 m x 3.0 m	340 kg	$3.3 \cdot 10^{-2}$
FP3-TE2	Diameter = 1.5 m Length = 0.7 m	80 kg	$6.9 \cdot 10^{-3}$

Table 5: Dimensions and weight of the fragments evaluated for each fragmentation pattern.

Given that the maximum number of fragments originated (N_F) is 3 for FP3, no more than 3 out of the 4 targets can be simultaneously affected by the primary scenario. Table 4 reports the number of possible combinations, where k targets are contemporary affected, as calculated by eq. (1). The table also reports the total number of domino scenarios for each fragmentation pattern (ν_{fp}) and the number of partial permutations fragment-target to be considered for each target combination ($\nu_{F,k}$). These figures have been calculated according to Eqs. (2) and (3) respectively. Table 4 reveals that, even in the simple case considered, the description of domino propagation by fragments may ask for the evaluation of a relevant number of different sub-cases, resulting by all the possible fragmentation patterns, configurations, and permutations of concern:

$$\nu_{TOT} = \sum_{fp=1}^{N_{fp}} \sum_{k=1}^{min(N_F,N_T)} (\nu_k \cdot \nu_{F,k}) = 112 \qquad (12)$$

An apparently similar situation (1 source and 4 targets), but involving a 'field-like' escalation vector (e.g. a blast wave) would have resulted in a smaller number of cases (15 when N_T=4 targets if the approach of [31] is considered).

The probability of generation ($P_{gen,F}$) for each of the 7 possible fragments identified in fragmentation pattern analysis was quantified according to eq.(4) (step 5.1). The probabilities to generate detached fragments after initial crack propagation (P_{cp}), the conditional probability of a specific fragmentation pattern producing that fragment (P_{fp}) and the probability of the given shape of the fragment (P_{fs}) were calculated starting from the procedure defined by Gubinelli et al. [2,49]. The results obtained are summarized in Table 6.

P_{cp}	fp	P_{fp}		P_{fs}	$P_{gen,j}$	$P_{imp,j->AB1}$	$P_{dam,j,AB1}$	$P_{j->AB1}$
0.90	FP1 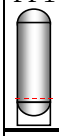	0.335	TE 	1.0	$3.02 \cdot 10^{-01}$	$4.60 \cdot 10^{-04}$	1.0	$1.39 \cdot 10^{-04}$
			PL 	1.0	$3.02 \cdot 10^{-01}$	0.00	1.0	0.00
	FP2 	0.335	TE	1.0	$3.02 \cdot 10^{-01}$	0.00	1.0	0.00
			PL 	1.0	$3.02 \cdot 10^{-01}$	$2.12 \cdot 10^{-03}$	1.0	$6.39 \cdot 10^{-04}$
	FP3 	0.230	TE1	1.0	$2.07 \cdot 10^{-01}$	$9.23 \cdot 10^{-04}$	1.0	$1.91 \cdot 10^{-04}$
			PL 	1.0	$2.07 \cdot 10^{-01}$	$4.81 \cdot 10^{-04}$	1.0	$9.96 \cdot 10^{-05}$
			TE2	1.0	$2.07 \cdot 10^{-01}$	0.00	1.0	0.00

P_{cp}: conditional probability of fragment detachment after initial crack propagation
fp: fragmentation pattern
P_{fp}: conditional probability of fragmentation pattern *fp*
P_{fs}: conditional probability of generation of a fragment of shape *fs*
$P_{gen,j}$: probability of generation of fragment *j*
$P_{imp,j->AB1}$: probability of impact of fragment *j* on target *AB1*
$P_{dam,j->AB1}$: damage probability after the impact of fragment *j* on target *AB1*
$P_{j->AB1}$: overall conditional probability of escalation considering the impact of fragment *j* on target *AB1*

Table 6: Probabilities of fragment generation from vessel AS2 and of escalation scenarios triggered by fragment impact in the case study.

The initial velocity of the fragment was estimated using the model of Baker et al. [50]. The fragments were classified according to the reference shapes described by Cozzani and Gubinelli [49] and the ballistic model by Gubinelli et al. [44] was applied to the evaluation of the probability of impact $P_{imp,j \to i}$ of the fragments on each target (step 5.2). Uniform probability distributions were used for the initial direction of projection, according to the findings by [78]. The main exception are the fragments originated by the lower portion of the vessel, for which no projection occurs due to initial direction of the

velocity [3], downwards impacting on the ground. An example of results is reported in Table 6 considering unit AB1 as target.

Probability of damage upon impact (step 6) was conservatively assumed to be 1. Similarly, the damage from the impact is conservatively assumed to cause the instantaneous loss of all the material and energy contained in the target unit.

For all the target units considered, the probability of escalation triggered by any fragment impacting on a given unit ($P_{j\rightarrow i}$) was calculated according to eq.(6). As an example, the results obtained for unit AB1 are reported in Table 6. It can be observed that the probability of escalation from some fragments results equal to zero. This is the consequence, confirmed by past accident data analysis [2] that some fragments, as discussed above, have an initial "downward" direction of projection, thus impacting on the ground.

In step 5.4 of the proposed methodology (see Figure 1), the probability of escalation calculated for single couples of fragments and targets ($P_{j\rightarrow i}$) were combined in order to obtain the probabilities of the domino scenarios. This was repeated for all the 112 cases identified by eq. (11). An example is provided in Figure 3, where the results obtained for the 3 cases of T_1^1 in FP3 are considered. The impact of fragments TE1, PL and TE2 of FP3 on target AB1 was assessed. The three permutations of interest are represented by matrices $q_{i,j,1}$ to $q_{i,j,3}$. The probabilities from $P_{q,1}$ to $P_{q,3}$ were calculated according to eq.(8). These were then combined according to eq.(10), in order to evaluate the probability to have a domino scenario affecting target AB1 (P_{T1}^{FP1}). As shown in Table 6, the probabilities of escalation ($P_{j\rightarrow i}$) are quite low. The application of the simplified evaluation described by eq.(9) would have resulted in very similar results for P_{T1}^{FP1}, with a relative error as low as 0.013%.

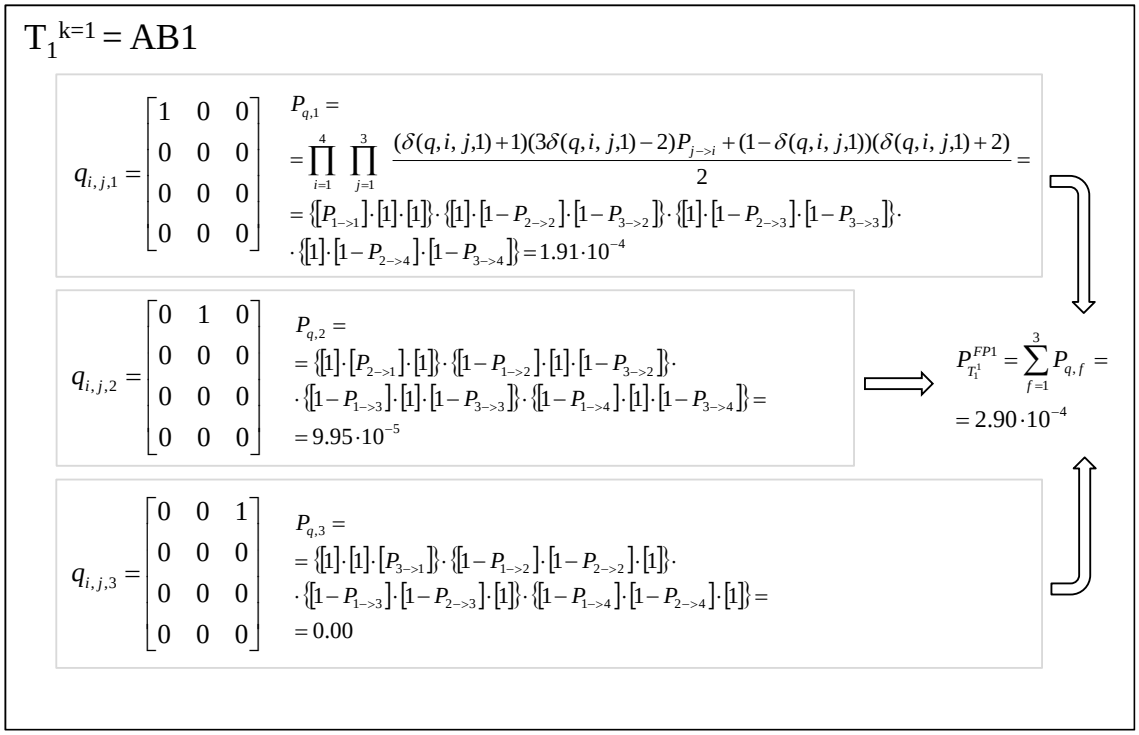

Figure 3: Example of calculation of the probability to have a domino scenario affecting only target AB1.

The same procedure presented in Figure 3 was repeated for the other combinations of targets (T_t^k) and for each fragmentation pattern, obtaining the results reported in table 7.

The table shows that scenarios involving multiple target damage are some orders of magnitude less probable than scenarios involving the failure of a single target. Moreover, since the projection of some fragments (i.e. those originating from the lower part of the vessel and projected downwards to the ground) was deemed not possible, the probabilities of the target combinations that require all the generated fragments to impact a target is zero. Actually, the fragments originating from the lower part of the vessel and ejected with a direction of the velocity that will cause their impact on the ground may be neglected in the assessment since the phase of characterization of the number of fragments in step 3.2 to reduce the computational requirements of the methodology.

It is also interesting to assess the overall probability that a target unit is impacted by any of the projected fragments. This may be calculated as:

$$P_{o,i} = \sum_{fp=1}^{N_{fp}} \sum_{j=1}^{N_F} \left(P_{gen,j} \cdot P_{imp,j\to i}\right) \quad (13)$$

Table 8 reports the results obtained. It can be observed that the values of $P_{o,i}$ are practically similar to the values of domino probability $P_{dom,T}$ for the k=1 scenarios affecting the same target (please remember that $P_{dam,j,i}$ is assumed here equal to 1, actually allowing this direct comparison). This suggests once more that the combinations involving multiple target damage provide only a negligible contribution to the probability of a target to be impacted.

K	T^k_t	P_T^{fp1}	P_T^{fp2}	P_T^{fp3}	$P_{dom,T}$	$f_{dom,T}$ [ev./y]
k=1	T^1_1 = AB1	$1.39 \cdot 10^{-04}$	$6.39 \cdot 10^{-04}$	$2.90 \cdot 10^{-04}$	$1.07 \cdot 10^{-03}$	$5.34 \cdot 10^{-08}$
	T^1_2 = AB2	$1.39 \cdot 10^{-04}$	$6.39 \cdot 10^{-04}$	$2.90 \cdot 10^{-04}$	$1.07 \cdot 10^{-03}$	$5.34 \cdot 10^{-08}$
	T^1_3 = AB3	$2.65 \cdot 10^{-04}$	$1.22 \cdot 10^{-03}$	$5.55 \cdot 10^{-04}$	$2.04 \cdot 10^{-03}$	$1.02 \cdot 10^{-07}$
	T^1_4 = AS1	$6.70 \cdot 10^{-05}$	$3.09 \cdot 10^{-04}$	$1.40 \cdot 10^{-04}$	$5.16 \cdot 10^{-04}$	$2.58 \cdot 10^{-08}$
k=2	T^2_1 =AB1+AB2	0.00	0.00	$3.80 \cdot 10^{-08}$	$3.80 \cdot 10^{-08}$	$1.90 \cdot 10^{-12}$
	T^2_2 =AB1+AB3	0.00	0.00	$7.26 \cdot 10^{-08}$	$7.26 \cdot 10^{-08}$	$3.63 \cdot 10^{-12}$
	T^2_3 =AB1+AS1	0.00	0.00	$1.84 \cdot 10^{-08}$	$1.84 \cdot 10^{-08}$	$9.19 \cdot 10^{-13}$
	T^2_4 =AB2+AB3	0.00	0.00	$7.26 \cdot 10^{-08}$	$7.26 \cdot 10^{-08}$	$3.63 \cdot 10^{-12}$
	T^2_5 =AB2+AS1	0.00	0.00	$1.84 \cdot 10^{-08}$	$1.84 \cdot 10^{-08}$	$9.19 \cdot 10^{-13}$
	T^2_6 =AB3+AS1	0.00	0.00	$3.51 \cdot 10^{-08}$	$3.51 \cdot 10^{-08}$	$1.75 \cdot 10^{-12}$
k=3	T^3_1 = AB1+AB2+AB3	N/A	N/A	0.00	0.00	0.00
	T^3_2 = AB1+AB2+AS1	N/A	N/A	0.00	0.00	0.00
	T^3_3 = AB1+AB3+AS1	N/A	N/A	0.00	0.00	0.00
	T^3_4 = AB2+AB3+AS1	N/A	N/A	0.00	0.00	0.00

T^k_t: *t-th* combination of *k* fragments impacting to *k* targets

P_T^{fp}: probability to have a domino scenario affecting the set T^k_t from the fragmentation pattern (*fp*)

$P_{dom,T}$: probability to have the domino scenario affecting the set T^k_t from any fragmentation pattern

$f_{dom,T}$: frequency of domino scenario affecting the set T^k_t from any fragmentation pattern

Table 7: Probabilities of domino scenario affecting the combinations of targets and resulting frequencies of domino scenarios in the case study.

Target	$P_{o,i}$
AB1	$1.07 \cdot 10^{-03}$
AB2	$1.07 \cdot 10^{-03}$
AB3	$2.04 \cdot 10^{-03}$
AS1	$5.16 \cdot 10^{-04}$

Table 8: Overall probabilities of fragment impact on the different target units in the lay out considered.

As discussed in section 2.4, short-cut assumptions are usually adopted in the description of target damage to a target and a single representative secondary scenario is selected for the sake of simplicity. Therefore, the overall probability of a domino scenario involving a given set of targets (T_t^k) can be obtained by eqs. (10) and (11). Table 6 presents the final results obtained by the assessment.

The final step (Step 10 in Figure 1) of the methodology concerns the calculation of risk indexes. The procedure is the same applied in the literature to other escalation vectors (see e.g. [31,86]).

In order to understand the modification in IR caused by fragment impact, some results are presented in the following for the scenarios involving the damage of target AB2 (permutation T_2^1). The secondary scenario expected from the damage of AB2 caused by fragment impact is the catastrophic failure of the vessel followed by a fireball. The physical consequences of the fireball were modeled according to TNO "Yellow Book" [79], and individual risk was calculated according to the probit model proposed in the TNO "Green Book" [87]. As shown in Table 6, the probability of this domino scenario is $1.07 \bullet 10^{-03}$, which combined with the frequency of the primary event (i.e. mechanical explosion of AS1, $f_P = 5 \bullet 10^{-05}$ ev/y) yields a frequency of the domino scenario equal to $5.34 \bullet 10^{-08}$ ev./y. It should be remarked that the frequency of the domino scenario is of the same order of magnitude of the frequency of the catastrophic failure from non-domino causes of the target vessel AB2, which was estimated in the general QRA study to be $2.48 \cdot 10^{-8}$ events/year. Considering that T_2^1 is not the sole domino propagation scenario possible for this target, the result evidences the importance to consider domino propagation by fragment projection in the QRA.

Figure 4-a shows the IR calculated for the primary scenario considered (catastrophic failure of vessel AS1 followed by a fireball). It should be remarked that, even if IR values below 10^{-10} events/year are usually considered negligible and not reported in IR maps, they were included in Figure 4-a to allow for an easier understanding of the contribute of the risk generated by domino effects due to fragment projection by comparison with Figures 4-b and 4-c. Figure 4-b shows the specific individual risk map calculated for the sole secondary scenario (catastrophic failure of vessel AB2 followed by a fireball) considering the frequency of the domino effect ($5.34 \bullet 10^{-08}$ ev./y). Figure 4-c reports the overall IR of the domino scenario (failure of vessel AS1 and fireball followed by failure of vessel AB2 and fireball).

The analysis of Figure 4 clearly shows the importance of considering domino effect caused by fragments and the escalation scenarios. As evident from the comparison of Figures 4-a and 4-c, important changes are present in the individual risk map when domino scenarios are considered. Even if the overall values of individual risk are low, confirming the low frequency of both scenarios involving the catastrophic failure of vessels and the impact of fragments, nevertheless the individual risk values are increased of several order of magnitude in the impact area considered when the domino scenario is considered.

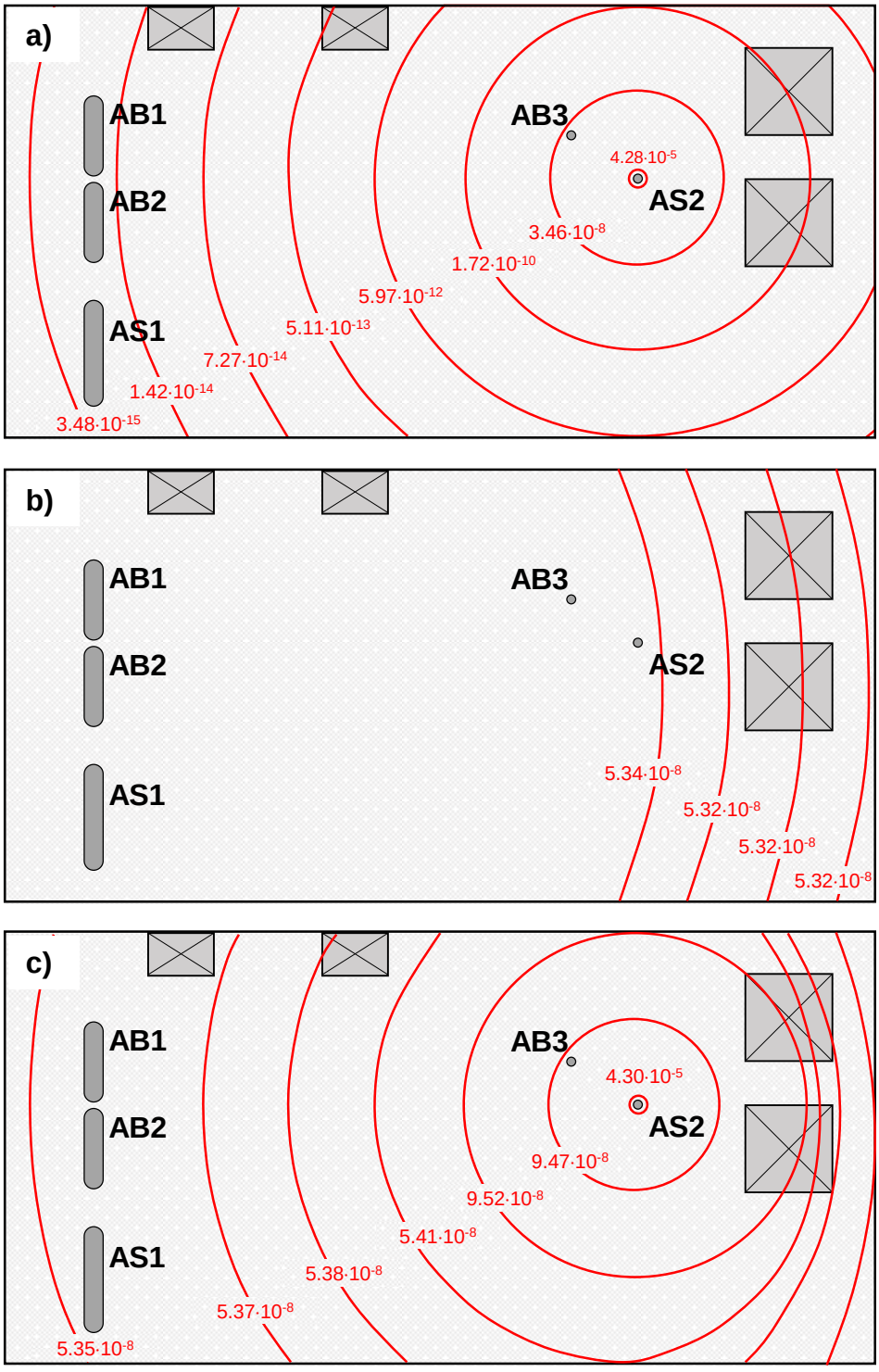

Figure 4: Local specific individual risk maps for selected scenarios: a) only primary scenario (blast wave) from AS2; b) only secondary scenario (fireball) from domino propagation of AS2 fragments on AB2; c) combined map of primary and secondary scenarios. All values of Individual Risk are expressed in events/year.

4.2 Benefits and limitations of the proposed method

The proposed method allows the integration of the propagation by fragment into the framework of the domino risk assessment. Particular attention was given to create a method compatible with an already existing procedure for domino risk assessment, in order to avoid the proliferation of stand-alone methods, which can possibly be less effective and more time consuming to use when a general quantitative assessment of risk related to domino scenarios is required [88,89].

The method specifically addresses the identification of possible fragment sources and the full quantification of the propagation probability. Moreover, it includes the assessment of the probability of fragment impact on multiple targets in the same event. The latter feature allows the analyst to quantify the relative weight of these high-impact low probability scenarios in terms of expected frequency, thus allowing on a case-by-case basis their inclusion or cut-off in the overall assessment.

The method is also suitable for automated application in consequence simulation software, as it does not require specific expert judgement for its application. Input data are common to other components of quantitative risk assessment procedures or are easily available from design documents.

The main epistemic limitations of the method arise from the simplification introduced to describe the size and number of fragments as well as the probability of escalation. In particular, the description of fragment shapes was based on a limited number of reference fragmentation patterns in order to limit the calculation effort. Though the patterns were proved to be representative of the outcomes of actual accidents and are supported on theoretical basis [2,90], they necessarily constitute only a discrete subset of the possible ones. The uncertainty on fragment shape, initial velocity and initial direction of the projected fragment obviously affects the description of the fragment flight and, therefore, the probability of impact. Also in these cases the assumptions and simplification in the models used were analyzed in the original references [31,44,49,78,79], confirming the reasonable performance of the models. Finally, the mentioned lack of reliable models allowing the description of the damage caused by fragment impact forces to introduce conservative assumptions in many practical cases (e.g. considering the probability of damage of the target, $P_{dam,j,i}$, equal to 1 and catastrophic failure of the target as presented in the case study). Future improvement of this part of the assessment are expected from the development of models relying on dynamic simulation, addressing specifically the impact of the projected fragment of process or storage equipment (e.g. Finite Element Methods) as well as field experiments.

5. Conclusions

A method for the quantitative assessment of domino effect and escalation caused by fragment impact was developed. The methodology addresses the calculation of escalation probabilities due to multiple fragment projection and the assessment of overall individual risk figures. The specific characteristics of fragment projection as an escalation vector, if compared to blast wave or thermal load, were assessed in detail: while the latter are "field-like" escalation vectors, escalation by fragments occurs by a "one-to-one" escalation mechanism. A fragment that impacts on a target cannot impact a target in a different spatial location, provided that the distances among the potential targets and between the fragment source and the targets are sufficiently large. Thus, the methodology developed allows assessing the influence of the number and direction of projected fragments on the possible escalation scenarios and on their probability.

Although the overall risk figures for this type of accident are expected to be lower than in the case of other accident scenarios as fires and toxic releases, an important increase in the individual risk was evidenced when considering domino scenarios caused by fragment projection if compared to the primary explosion scenario, evidencing how fragment projection may play a significant role in triggering escalation. Thus, the procedure developed, allowing for a detailed quantitative assessment of these scenarios, may play an important role in the correct assessment and management of risk due to domino accidents triggered by fragment projection.

REFERENCES

[1] Lees' Loss Prevention in the Process Industries. Elsevier; 2005. https://doi.org/10.1016/B978-0-7506-7555-0.50272-3.

[2] Gubinelli G, Cozzani V. Assessment of missile hazards: Identification of reference fragmentation patterns. J Hazard Mater 2009;163:1008–18. https://doi.org/10.1016/j.jhazmat.2008.07.056.

[3] Tugnoli A, Cozzani V, Khan F, Amyotte P. Missile Projection Effects. In Domino Effects in the Process Industries: Modelling, Prevention and Managing The Netherlands: Elsevier; 2013. https://doi.org/10.1016/B978-0-444-54323-3.00006-3.

[4] Chen C, Reniers G, Khakzad N. A thorough classification and discussion of approaches for modeling and managing domino effects in the process industries. Safety Science 2020; 125: 104618. https://doi.org/10.1016/j.ssci.2020.104618.

[5] Khakzad N, Reniers G. Using graph theory to analyze the vulnerability of process plants in the context of cascading effects. Reliab Eng Syst Saf 2015;143:63–73. https://doi.org/10.1016/j.ress.2015.04.015.

[6] Khan F, Abbasi SA. Models for domino effect analysis in chemical process industries. Process Saf Prog 1998;17:107–23. https://doi.org/10.1002/prs.680170207.

[7] Bagster DF, Pitblado RM. Estimation of domino incident frequencies - an approach. Process Saf Environ Prot Trans Inst Chem Eng Part B 1991;69:195–9.

[8] CCPS - Center of Chemical Process Safety. Guidelines for chemical process quantitative risk analysis. New York: American Institute of Chemical Engineers - Center of Chemical Process Safety; 2000.

[9] Gledhill J, Lines I. Development of methods to assess the significance of domino effects from major hazard sites. CR Report 183, Health and Safety Executive.

[10] Shen C, Ma L, Huang G, Wu Y, Zheng J, Liu Y, et al. Consequence assessment of high-pressure hydrogen storage tank rupture during fire test. J Loss Prev Process Ind 2018;55:223–31. https://doi.org/10.1016/j.jlp.2018.06.016.

[11] Sun D, Sun J, Li Z, Jiang J, Zhang M, Wang Z. Investigation of the influence of the projected proportion of a burst vessel on the hazard caused by fragments. J Loss Prev Process Ind 2019;62:103975. https://doi.org/10.1016/j.jlp.2019.103975.

[12] Hemmatian B, Planas E, Casal J. Comparative analysis of BLEVE mechanical energy and overpressure modelling. Process Saf Environ Prot 2017;106:138–49. https://doi.org/10.1016/j.psep.2017.01.007.

[13] Jiang D, Pan XH, Hua M, Mébarki A, Jiang JC. Assessment of tanks vulnerability and domino effect analysis in chemical storage plants. J Loss Prev Process Ind 2019;60:174–82. https://doi.org/10.1016/j.jlp.2019.04.016.

[14] Abdolhamidzadeh B, Hassan CRC, Hamid MD, Farrokhmehr S, Badri N, Rashtchian D. Anatomy of a domino accident: Roots, triggers and lessons learnt. Process Saf Environ Prot 2012;90:424–9. https://doi.org/10.1016/j.psep.2012.04.003.

[15] Abdolhamidzadeh B, Abbasi T, Rashtchian D, Abbasi SA. Domino effect in process-industry accidents - An inventory of past events and identification of some patterns. J Loss Prev Process Ind 2011;24:575–93.

https://doi.org/10.1016/j.jlp.2010.06.013.
[16] Misuri A, Antonioni G, Cozzani V. Quantitative risk assessment of domino effect in Natech scenarios triggered by lightning. J Loss Prev Process Ind 2020;64:104095. https://doi.org/10.1016/j.jlp.2020.104095.
[17] Khan FI, Abbasi SA. Major accidents in process industries and an analysis of causes and consequences. J Loss Prev Process Ind 1999;12:361–78. https://doi.org/10.1016/S0950-4230(98)00062-X.
[18] Pietersen CM. Analysis of the LPG-disaster in mexico city. J Hazard Mater 1988;20:85–107. https://doi.org/10.1016/0304-3894(88)87008-0.
[19] Wang B, Wu C, Kang L, Reniers G, Huang L. Work safety in China's Thirteenth Five-Year plan period (2016--2020): Current status, new challenges and future tasks. Saf Sci 2018;104:164–78. https://doi.org/10.1016/j.ssci.2018.01.012.
[20] Chen C, Reniers G, Khakzad N. Integrating safety and security resources to protect chemical industrial parks from man-made domino effects: a dynamic graph approach. Reliab Eng \& Syst Saf 2019;191:106470. https://doi.org/10.1016/j.ress.2019.04.02
[21] Ding L, Khan F, Abbassi R, Ji J. FSEM: An approach to model contribution of synergistic effect of fires for domino effects. Reliab Eng Syst Saf 2019;189:271–8. https://doi.org/10.1016/j.ress.2019.04.041.
[22] Zeng T, Chen G, Yang Y, Chen P, Reniers G. Developing an advanced dynamic risk analysis method for fire-related domino effects. Process Saf Environ Prot 2020;134:149–60. https://doi.org/10.1016/j.psep.2019.11.029
[23] Zhang M, Zheng F, Chen F, Pan W, Mo S. Propagation probability of domino effect based on analysis of accident chain in storage tank area. J Loss Prev Process Ind 2019;62:103962. https://doi.org/10.1016/j.jlp.2019.103962
[24] Huang K, Chen G, Khan F, Yang Y. Dynamic analysis for fire-induced domino effects in chemical process industries. Process Saf Environ Prot 2021;148:686–97. https://doi.org/10.1016/j.psep.2021.01.042.
[25] Codetta-Raiteri D, Bobbio A, Montani S, Portinale L. A dynamic Bayesian network based framework to evaluate cascading effects in a power grid. Eng Appl Artif Intell 2012;25:683–97. https://doi.org/10.1016/j.engappai.2010.06.005.
[26] Bentes I, Afonso L, Varum H, Pinto J, Varajão J, Duarte A, et al. A new tool to assess water pipe networks vulnerability and robustness. Eng Fail Anal 2011;18:1637–44. https://doi.org/10.1016/j.engfailanal.2011.01.002.
[27] Necci A, Cozzani V, Spadoni G, Khan F. Assessment of domino effect: State of the art and research Needs. Reliab Eng Syst Saf 2015;143:3–18. https://doi.org/10.1016/j.ress.2015.05.017.
[28] Khakzad N. Application of dynamic Bayesian network to risk analysis of domino effects in chemical infrastructures. Reliab Eng Syst Saf 2015;138:263–72. https://doi.org/10.1016/j.ress.2015.02.007.
[29] Landucci G, Necci A, Antonioni G, Argenti F, Cozzani V. Risk assessment of mitigated domino scenarios in process facilities. Reliab Eng Syst Saf 2017;160:37–53. https://doi.org/10.1016/j.ress.2016.11.023.
[30] Ding L, Khan F, Ji J. A novel approach for domino effects modeling and risk analysis based on synergistic effect and accident evidence. Reliab Eng Syst Saf 2020;203:107109. https://doi.org/10.1016/j.ress.2020.107109.

[31] Cozzani V, Gubinelli G, Antonioni G, Spadoni G, Zanelli S. The assessment of risk caused by domino effect in quantitative area risk analysis. J Hazard Mater 2005;127:14–30. https://doi.org/10.1016/j.jhazmat.2005.07.003.
[32] Khan FI, Abbasi SA. Simulation of accidents in a chemical industry using the software package MAXCRED. Indian J Chem Technol 1996;3:338–44.
[33] Khan FI, Abbasi SA. DOMIFFECT (DOMIno eFFECT): User-friendly software for domino effect analysis. Environ Model Softw 1998;13:163–77. https://doi.org/10.1016/S1364-8152(98)00018-8.
[34] Cozzani V, Gubinelli G, Salzano E. Escalation thresholds in the assessment of domino accidental events. J Hazard Mater 2006;129:1–21. https://doi.org/10.1016/j.jhazmat.2005.08.012.
[35] Alileche N, Cozzani V, Reniers G, Estel L. Thresholds for domino effects and safety distances in the process industry: A review of approaches and regulations. Reliab Eng Syst Saf 2015;143:74–84. https://doi.org/10.1016/j.ress.2015.04.007.
[36] BBC News. Spanish chemical plant explosion kills man 3km away. BBC 2020. https://www.bbc.com/news/world-europe-51113132 (accessed April 22, 2021).
[37] Cozzani V, Tugnoli A, Salzano E. Prevention of domino effect: From active and passive strategies to inherently safer design. J Hazard Mater 2007;139:209–19. https://doi.org/10.1016/j.jhazmat.2006.06.041.
[38] Cozzani V, Tugnoli A, Salzano E. The development of an inherent safety approach to the prevention of domino accidents. Accid Anal Prev 2009;41:1216–27. https://doi.org/10.1016/j.aap.2008.06.002.
[39] Tugnoli A, Cozzani V, Khan F, Amyotte P. Managing Domino Effects from a Design-Based Viewpoint. Elsevier B.V.; 2013. https://doi.org/10.1016/B978-0-444-54323-3.00012-9.
[40] Baker WE. Blast and fragments from bursting pressure vessels. Am. Soc. Mech. Eng. Press. Vessel. Pip. Div. PVP, vol. 82, 1984, p. 51–66.
[41] Sun D, Jiang J, Zhang M, Wang Z, Zhang Y, Cai L. Investigation of multiple domino scenarios caused by fragments. J Loss Prev Process Ind 2016;40:591–602. https://doi.org/10.1016/j.jlp.2016.01.023.
[42] Hauptmanns U. A Monte-Carlo based procedure for treating the flight of missiles from tank explosions. Probabilistic Eng Mech 2001;16:307–12. https://doi.org/10.1016/S0266-8920(01)00023-6.
[43] Hauptmanns U. A procedure for analyzing the flight of missiles from explosions of cylindrical vessels. J Loss Prev Process Ind 2001;14:395–402. https://doi.org/10.1016/S0950-4230(01)00011-0.
[44] Gubinelli G, Zanelli S, Cozzani V. A simplified model for the assessment of the impact probability of fragments. J Hazard Mater 2004;116:175–87. https://doi.org/10.1016/j.jhazmat.2004.09.002.
[45] Mébarki A, Mercier F, Nguyen QB, Saada RA. Structural fragments and explosions in industrial facilities. Part I: Probabilistic description of the source terms. J Loss Prev Process Ind 2009;22:408–16. https://doi.org/10.1016/j.jlp.2009.02.006.
[46] Mébarki A, Nguyen QB, Mercier F. Structural fragments and explosions in industrial facilities: Part II - Projectile trajectory and probability of impact. J Loss Prev Process Ind 2009;22:417–25. https://doi.org/10.1016/j.jlp.2009.02.005.
[47] Holden PL, Reeves AB. Fragment hazards from failures of pressurised liquefied

gas vessels. Inst. Chem. Eng. Symp. Ser., 1985, p. 205–20.
[48] Westin RA. Summary of Ruptured Tank Cars Involved in Past Accidents. 1971.
[49] Gubinelli G, Cozzani V. Assessment of missile hazards: Evaluation of the fragment number and drag factors. J Hazard Mater 2009;161:439–49. https://doi.org/10.1016/j.jhazmat.2008.03.116.
[50] Baker WE, Cox PA, Kulesz JJ, Strehlow RA, Westine PS. Explosion hazards and evaluation. Elsevier; 2012.
[51] Baum MR. The velocity of missiles generated by the disintegration of gas - Pressurized vessels and pipes. J Press Vessel Technol Trans ASME 1984;106:362–8. https://doi.org/10.1115/1.3264365.
[52] Baum MR. Disruptive failure of pressure vessels: Preliminary design guidelines for fragment velocity and the extent of the hazard zone. J Press Vessel Technol Trans ASME 1988;110:168–76. https://doi.org/10.1115/1.3265582.
[53] Gel'fand BE, Frolov SM, Bartenev AM. Calculation of the rupture of a high-pressure reactor vessel. Combust Explos Shock Waves 1988;24:488–96. https://doi.org/10.1007/BF00750027.
[54] Moore C V. The design of barricades for hazardous pressure systems. Nucl Eng Des 1967;5:81–97. https://doi.org/10.1016/0029-5493(67)90081-7.
[55] Vaidogas ER. Predicting the ejection velocities of fragments from explosions cylindrical pressure vessels: Uncertainty and sensitivity analysis. J Loss Prev Process Ind 2021;71:104450. https://doi.org/10.1016/j.jlp.2021.104450.
[56] Nguyen QB, Mebarki A, Saada RA, Mercier F, Reimeringer M. Integrated probabilistic framework for domino effect and risk analysis. Adv Eng Softw 2009;40:892–901. https://doi.org/10.1016/j.advengsoft.2009.01.002.
[57] Pula R, Khan FI, Veitch B, Amyotte PR. A model for estimating the probability of missile impact: Missiles originating from bursting horizontal cylindrical vessels. Process Saf Prog 2007;26:129–39. https://doi.org/10.1002/prs.10178.
[58] Neilson AJ. Empirical equations for the perforation of mild steel plates. Int J Impact Eng 1985;3:137–42. https://doi.org/10.1016/0734-743X(85)90031-4.
[59] Ohte S, Yoshizawa H, Chiba N, Shida S. Impact Strength of Steel Plates Struck by Projectiles: Evaluation Formula for Critical Fracture Energy of Steel Plate. Bull JSME 1982;25:1226–31.
[60] Stronge WJ. Impact and perforation of cylindrical shells by blunt missiles. In: REID SR, editor. Met. Form. Impact Mech., Pergamon; 1985, p. 289–302. https://doi.org/https://doi.org/10.1016/B978-0-08-031679-6.50024-2.
[61] Baker WE, Kulesz JJ, Ricker RE, Bessey RL, Westline PS. Workbook for predicting pressure wave and fragment effect of exploding propellent tanks and gas storage vessels. 1975.
[62] Kar AK. Residual velocity for projectiles. Nucl Eng Des 1979;53:87–95. https://doi.org/https://doi.org/10.1016/0029-5493(79)90042-6.
[63] Neilson AJ, Howe WD, Garton GP. Impact resistance of mild steel pipes: an experimental study. 1987.
[64] Cox BG, Saville G. High pressure safety code 1975.
[65] Recht R, Ipson TW. Ballistic perforation dynamics 1963.
[66] Resistance of various metallic materials to preforation by steel fragments; empirical relationships for fragments residual velocity and residual weight. Technical Report, Johns Hopkins Univ., Cockeysville, MD. Ballistic Analysis

Lab., Maryl 1961.
[67] Ellinas CP. Damage on offshore tubular bracing member. IABSE colloquium, Copenhagen, 1983, vol. 42, 1983, p. 253–61.
[68] Westine PS, Vargas LM. Design Guide for Armoring Critical Aircraft Components to Protect from High Explosive Projectiles, Final Report. Contract 1978.
[69] Lisi R, Consolo G, Maschio G, Milazzo MF. Estimation of the impact probability in domino effects due to the projection of fragments. Process Saf Environ Prot 2015;93:99–110. https://doi.org/10.1016/j.psep.2014.05.003.
[70] Reniers G, Cozzani V. Domino Effects in the Process Industries: Modelling, Prevention and Managing. Elsevier B.V.; 2013. https://doi.org/10.1016/C2011-0-00004-2.
[71] Reniers G, Cozzani V, Landucci G, Salzano E, Taveau J, Spadoni G, et al. Domino Effects in the Process Industries. Amsterdam, The Netherlands: Elsevier; 2013.
[72] Cozzani V, Antonioni G, Khakzad N, Khan F, Taveau J, Reniers G. Quantitative Assessment of Risk Caused by Domino Accidents. Domino Eff. Process Ind. Model. Prev. Manag., Elsevier B.V.; 2013, p. 208–28. https://doi.org/10.1016/B978-0-444-54323-3.00010-5.
[73] of Chemical Engineers AI, Company DC. Fire & Explosion Index: Hazard Classification Guide. Amer Inst of Chemical Engineers; 1987.
[74] Fingas MF. The handbook of hazardous materials spills technology. McGraw-Hill; 2002.
[75] Djelosevic M, Tepic G. Identification of fragmentation mechanism and risk analysis due to explosion of cylindrical tank. J Hazard Mater 2019;362:17–35. https://doi.org/10.1016/j.jhazmat.2018.09.013.
[76] Djelosevic M, Tepic G. Probabilistic simulation model of fragmentation risk. J Loss Prev Process Ind 2019;60:53–75. https://doi.org/10.1016/j.jlp.2019.04.003.
[77] Sun D, Jiang J, Zhang M, Wang Z, Zhang Y, Yan L, et al. Investigation on the approach of intercepting fragments generated by vessel explosion using barrier net. J Loss Prev Process Ind 2017;49:989–96. https://doi.org/10.1016/j.jlp.2016.10.012.
[78] Tugnoli A, Gubinelli G, Landucci G, Cozzani V. Assessment of fragment projection hazard: Probability distributions for the initial direction of fragments. J Hazard Mater 2014;279:418–27. https://doi.org/10.1016/j.jhazmat.2014.07.034.
[79] van den Bosch CJH, Weterings RAP. Methods for the Calculation of Physical Effects Due to releases of hazardous materials (liquids and gases) “Yellow Book.” Tno Cpr 14E 2005:6.1-6.132.
[80] Baum MR. Velocity of missiles generated by the disintegration of gas pressurised vessels and pipes. Am. Soc. Mech. Eng. Press. Vessel. Pip. Div. PVP, vol. 82, 1984, p. 67–83.
[81] Gwaltney RC. Missile generation and protection in light-water-cooled power reactor plants. 1968.
[82] Chen G, Zhao Y, Xue Y, Huang K, Zeng T. Numerical investigation on performance of protective layer around large-scale chemical storage tank against impact by projectile. J Loss Prev Process Ind 2021;69. https://doi.org/10.1016/j.jlp.2020.104351.

[83] Sun D, Jiang J, Zhang M, Wang Z. Ballistic experiments on the mechanism of protective layer against domino effect caused by projectiles. J Loss Prev Process Ind 2016;40:17–28. https://doi.org/10.1016/j.jlp.2015.11.020.
[84] TNO. Guidelines for quantitative risk assessment (Purple Book). Sdu ùuitgevers; 2005.
[85] Hurst NW, Nussey C, Pape RP. Development and application of a risk assessment tool (RISKAT) in the heath and safety executive. Chem Eng Res \& Des 1989;67:362–72.
[86] Cozzani V, Tugnoli A, Bonvicini S, Salzano E. Threshold-Based Approach. Domino Eff. Process Ind., Amsterdam, The Netherlands: Elsevier Inc. Chapters; 2013, p. 189–207. https://doi.org/10.1016/B978-0-444-54323-3.00009-9.
[87] TNO. PSG1: Methods for Determining of Possible Damage to People and Objects Resulting from Releases of Hazardous Materials (green book). Publ Ser Danger Subst 2005.
[88] Nadia C, Catalin R. The Role of Standardization in Improving the Effectiveness of Integrated Risk Management. Adv. Risk Manag., IntechOpen; 2010. https://doi.org/10.5772/9893.
[89] Brocal F, González C, Sebastián MA, Reniers GLL, Paltrinieri N. Standardized risk assessment techniques: A review in the framework of occupational safety. Saf Reliab Soc a Chang World 2018:2889–95.
[90] Tugnoli A, Milazzo MF, Landucci G, Cozzani V, Maschio G. Assessment of the hazard due to fragment projection: A case study. J Loss Prev Process Ind 2014;28:36–46. https://doi.org/10.1016/j.jlp.2013.08.015.